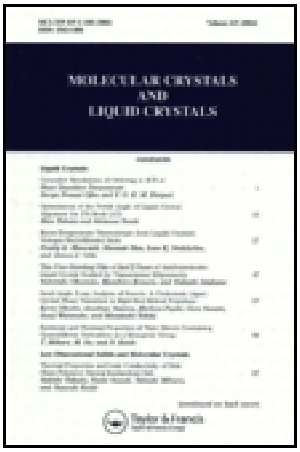

Molecular Crystals and Liquid Crystals Science and Technology. Section A. Molecular Crystals and Liquid Crystals

Publication details, including instructions for authors and subscription information:
http://www.tandfonline.com/loi/gmcl19

Binary Phase Diagram with Non Isomorphous n-Alkanes: $C_{12}H_{26}6$ - $C_{15}H_{32}$. Implication of the Rotator Phase R, in the Melting Behaviour of Odd - Even and Even - Odd Phase Diagrams

P. Espeau [a], F. Rajabalee [a] & Y Haget [a]

[a] Centre de Physique Moléculaire Optique et Hertzienne, UMR 5798 au CNRS, 351 Cours de la Libération, Université Bordeaux l, 33405, Talence Cédex, France

To cite this article: P. Espeau, F. Rajabalee & Y Haget (1998): Binary Phase Diagram with Non Isomorphous n-Alkanes: $C_{12}H_{26}6$ - $C_{15}H_{32}$. Implication of the Rotator Phase R, in the Melting Behaviour of Odd - Even and Even - Odd Phase Diagrams, Molecular Crystals and Liquid Crystals Science and Technology. Section A. Molecular Crystals and Liquid Crystals, 323:1, 145-153

To link to this article: http://dx.doi.org/10.1080/10587259808048438

Mol. Cryst. Liq. Cryst., Vol. 323, pp. 145–153
Reprints available directly from the publisher
Photocopying permitted by license only

Binary Phase Diagram with Non Isomorphous *n*-Alkanes: $C_{12}H_{26}$ – $C_{15}H_{32}$. Implication of the Rotator Phase R_I in the Melting Behaviour of Odd – Even and Even – Odd Phase Diagrams

P. ESPEAU*, F. RAJABALEE and Y. HAGET

Centre de Physique Moléculaire Optique et Hertzienne, UMR 5798 au CNRS, 351 Cours de la Libération, Université Bordeaux I, 33405 Talence Cédex, France

(Received 28 February 1998)

The phase diagram of n-$C_{12}H_{26}+n$-$C_{15}H_{32}$ established by calorimetric and X-ray diffraction analyses exhibits no less than four single phase domains [T_{12}], [O_{15}], [Ri_{15}] and [L], two invariants: a eutectic at $T=258.3$ K and a metatectic at $T=263.3$ K, and five two-phase domains. From a thermodynamic point of view, an interpretation of the phase diagram is given and an attempt is undertaken to modelise the [R_I + L] equilibrium. The extent in composition x of this phase as well as the width in temperature of the [R_I + L] eutectic at $x=1/2$, are explained in terms of degree of isomorphism $\varepsilon^{i}_{m}(R_I)$ and excess Gibbs energy functions $G^{E,\mathrm{sol}}(x)$. Those quantities as well as the melting temperature difference (ΔT) at $x=1/2$, are compared and discussed with other binary systems.

Keywords: *n*-dodecane; *n*-pentadecane; phase diagram; crystallographic and thermodynamic analyses; degree of isomorphism

I. INTRODUCTION

We have shown in previous papers [1–3] that when binary phase diagrams of alkanes C_nH_{2n+2} with $8 \leq n \leq 21$ and having the same parity are considered, complete miscibility is obtained only in the case of the odd–odd systems

---

*Corresponding author.

with a chain length difference (Δn) equal to 2. In other cases, even–even ($\Delta n = 2$) or odd–odd systems with $\Delta n > 2$, the miscibility is very narrow. For even–odd or odd–even systems [4], wide domains of miscibility in R_I form are present before melting. This rotator phase R_I, Face Centred Orthorhombic, is stable before melting in the odd-numbered carbon alkanes and metastable in the even ones. Apart from $C_8H_{18}-C_{10}H_{22}$ [2], the R_I form is also stabilised in the even–even binary phase diagram [4].

The phase diagram presented here is a special case since it is an even–odd system with $\Delta n = 3$ instead of 1 in the previous examples. After presenting the establishment of the phase diagram, the implication of the R_I phase in the melting behaviour will be shown. A thermodynamic assessment is performed for the determination of the primary binary phase diagram of this R_I form using known thermodynamic and crystallographic data from binary systems with $\Delta n = 1$ or 2.

II. EXPERIMENTAL

The commercial products are used without further purification and the purity grade is 99.1% for $C_{12}H_{26}$ and 99.4% for $C_{15}H_{32}$.

In the following paper, for more convenience, the alkanes will be named C_n instead of C_nH_{2n+2}.

A Guinier–Simon camera was used to observe, for a given mole fraction, the phase transitions as a function of temperature and to precise the number and the nature of the phases in presence.

A Perkin-Elmer DSC7 was used to observe the different endothermic phenomena. The temperatures are obtained using the form factor method [5]. More details about the methods used are given elsewhere [1, 2, 4].

III. PROPERTIES OF THE PURE COMPONENTS

The C_{12}, like the other even-numbered-carbon compounds until C_{24}, presents a triclinic structure, $P\bar{1}$, with one molecule per unit cell, before melting. The cell parameters are given in Table I.

The C_{15}, as the other odd-numbered-carbon alkanes between C_{13} and C_{21}, presents one solid–solid transition before melting. The low temperature form is orthorhombic Pbcm with four molecules per unit cell ($Z = 4$). The high temperature form is Faced Centred Orthorhombic Fmmm with $Z = 4$; this phase is also called rotator phase R_I [6].

TABLE I Cell parameters for the pure components C_{12} and C_{15}. (T_a: analysis temperature)

	$a(\AA)$	$b(\AA)$	$c(\AA)$	$\alpha(°)$	$\beta(°)$	$\gamma(°)$	$T_a(K)$
C_{12}	4.30 ± 0.01	4.79 ± 0.01	16.42 ± 0.06	81.3 ± 0.6	65.6 ± 0.2	73.8 ± 0.3	253
C_{15} (O)	4.99 ± 0.01	7.43 ± 0.02	42.3 ± 0.1	90	90	90	263
C_{15} (R_I)	5.13 ± 0.02	7.69 ± 0.01	42.3 ± 0.2	90	90	90	278

TABLE II Energetic characteristics of the pure components C_{12} and C_{15}

	$T(K)$	$\Delta H(kJ/mol)$
C_{12} (T → L)	263.1 ± 0.8	35.7 ± 0.7
C_{15} (O → R_I)	270.3 ± 0.8	8.7 ± 0.6
C_{15} (R_I → L)	282.7 ± 0.8	34.2 ± 2.4

With temperature, the parameters remain practically constant for C_{12} in the triclinic phase. On the other hand, for C_{15}, *a*, *b* and *c* parameters are virtually constant with temperature in the orthorhombic O phase while, in the R_I phase, *a* increases and *b* decreases. However, the cell volume does not change too much in this rotator phase [7].

The temperatures and enthalpies of phase transitions in C_{12} and C_{15} are given in Table II.

IV. PHASE DIAGRAM

As we told before, we investigated energetic and crystallographic methods to determine this phase diagram. These results are reported on Figure 1. Two invariants are found, the first one corresponds to a eutectic the energetic characteristics of which are as follows:

$$T_E = (258.3 \pm 0.3)\,\mathrm{K}$$
$$x_K = 0.07, \quad x_L \approx 0.24 \quad \text{and} \quad x_M \approx 0.94, \quad \text{in } C_{15}$$

and the second invariant presented by this phase diagram is a metatectic:

$$T_M = (263.3 \pm 0.3)\,\mathrm{K}$$
$$x_{K'} = 0.32, \quad x_{L'} \approx 0.61 \quad \text{and} \quad x_{M'} \approx 0.95, \quad \text{in } C_{15}.$$

The miscibility is very narrow from each side of the diagram. Three monophased regions are issued from those ones of the pure components:

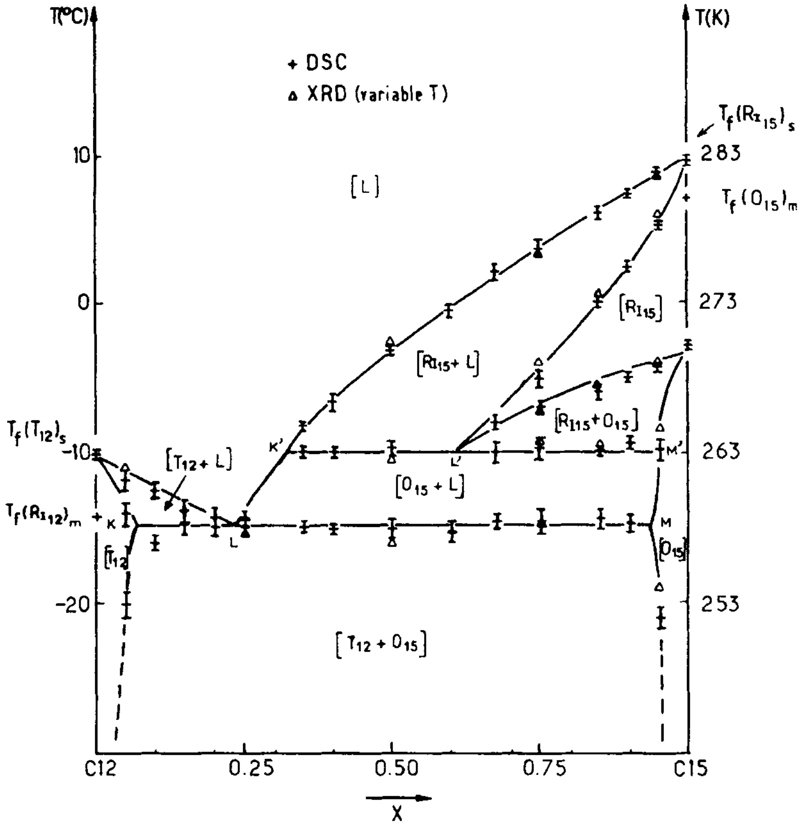

FIGURE 1 T-X phase diagram of the $C_{12}-C_{15}$ system.

- one, triclinic, coming from C_{12}
- an orthorhombic O and a rotator phase R_I coming from C_{15}. The latter is the widest one.

V. THERMODYNAMIC INTERPRETATION. MODELISATION OF THE PRIMARY PHASE DIAGRAM OF THE R_I PHASE

V.I. Thermodynamic Interpretation

From a thermodynamic point of view, we can explain the eutectic invariant by the intersection of the melting loop of the triclinic form of the C_{12} and the melting loop of the O_{15} form. The $O_{15} \to L$ transition is purely metastable (noted by m in subscript). To obtain its thermodynamic characteristics, we use the Hess Law, thus:

$$T_f(\mathrm{O}_{15})_m = 280.1\,\mathrm{K}$$
$$\Delta S_f(\mathrm{O}_{15})_m = 153\,\mathrm{J\cdot mol^{-1}\cdot K^{-1}}$$

As for the metatectic invariant, we can interpret its existence as the intersection between the [Ri_{15} + L] domain and [O_{15} + L].

This kind of thermodynamic reasoning from metastable states is very useful for the thermodynamic modelisation where we need to perform calculations in relation to the liquid state as a reference state (most of the time considered as an ideal state). But, we can also argue with only stable phases as well. And in this case, the metatectic invariant will be the intersection of the [Ri_{15} + L] domain and the [O_{15} + Ri_{15}] domain.

As said in the introduction, the $\mathrm{R_I}$ phase is predominantly present in all the studied binary systems ($\Delta n = 1$ and 2) in the range C_8 to C_{21}. That is why this phase presents a special interest in our study. Extraction of the primary [$\mathrm{R_I}$ + L] phase diagrams from the global ones is necessary to understand the implication of this phase in the melting behaviour over the whole range of phase diagrams. To do this, we perform thermodynamic assessment using thermodynamic data of the pure components in the $\mathrm{R_I}$ form (stable for the odd alkane but metastable for the even one).

To determine the energetic characteristics (T_f and ΔH_f) for the even-numbered-carbon alkanes crystallising in the $\mathrm{R_I}$ form, we can get these values from the data relative to the odd ones [4], thus:

$$T_f(\mathrm{Ri}_{12})_m = 258.3\,\mathrm{K}$$
$$\Delta H_f(\mathrm{Ri}_{12})_m = 25.8\,\mathrm{kJ\cdot mol^{-1}}.$$

V.II. Modelisation

In the following, several hypotheses were considered for the modelisation using the LIQFIT program [8]: the ΔC_p of the pure components and the excess Gibbs energy in the liquid state are neglected. The thermodynamic quantity calculated by LIQFIT (a procedure based upon the Equal-G-Curve concept [9]) is the excess Gibbs energy difference (ΔG^E) expressed as:

$$\Delta G^E(x,T) = G^{E,\mathrm{liq}}(x,T) - G^{E,\mathrm{sol}}(x,T)$$

where x is the mole fraction, T the temperature and sol is for the $\mathrm{R_I}$ phase.

Generally, the excess enthalpy and entropy differences are virtually constant over a wide range of temperature [10, 11]. Taking into account the above hypotheses, we obtain:

$$\Delta G^E(x,T) \approx \Delta G^E(x,T_m) = \Delta H^E(x) - T_m \Delta S^E(x)$$

where T_m is the mean temperature (for a given binary system) of the solid-to-liquid transition. On expanding the above relation, we get:

$$\Delta G^E(x,T_m) = H^{E,\mathrm{liq}}(x) - T_m S^{E,\mathrm{liq}}(x) - (H^{E,\mathrm{sol}}(x) - T_m S^{E,\mathrm{sol}}(x))$$

Neglecting excess quantities of the liquid, we obtain:

$$\Delta G^E(x,T_m) = -H^{E,\mathrm{sol}}(x) - T_m S^{E,\mathrm{sol}}(x) \qquad (1)$$

Excess enthalpy in the solid state is easy to obtain when the domain in concentration of the R_I phase is wide enough. This is usually the case for binary systems with $\Delta n = 1$ or 2. For our system, only 40% of solidus–liquidus (R_I–L) pairs are accessible experimentally, which is not enough to enable the calculation of the excess enthalpy in the R_I form. So, to evaluate this excess quantity, we use thermodynamic correlations previously done on binary phase diagrams of *n*-alkanes with $\Delta n = 1$ or 2 [11].

Oonk *et al.* [11] show that the variation of the excess enthalpy $H^{E,\mathrm{sol}}(x = 1/2)$ is linear with $\Delta n/\bar{n}$, where Δn is the carbon difference between the two components of the binary system and $\bar{n}$ is the average of the number of carbons between those molecules (in our case $\bar{n} = 13.5$). From this curve, we get $H^{E,\mathrm{sol}}(x = 1/2) = 5000\,\mathrm{J \cdot mol^{-1}}$ for the C_{12}–C_{15} system. $S^{E,\mathrm{sol}}$ is calculated from the relation $S^{E,\mathrm{sol}} = \theta \cdot H^{E,\mathrm{sol}}$, where θ is the compensation temperature [10]. With those values, and using Eq. (1), we get $G^{E,\mathrm{sol}}(x = 1/2) = 800\,\mathrm{J \cdot mol^{-1}}$. The calculation of the diagram with those values lead to a narrow eutectic displaced towards the C_{12} component. However, we note a deviation from the experimental points for the mean compositions that we can explain by the incidence of the O phase which is not considered in this part. Nevertheless, the liquidus curve (in the stable part) is well fitted.

VI. DISCUSSION

The cell parameters of C_{12} and C_{15} reported in Table III enable us to calculate the degree of isomorphism in the R_I phase $\varepsilon^i_m(R_I)$ the definition of

TABLE III Cell parameters of C_{12} (metastable) and C_{15} (stable) of the R_I phase (mean values), (data of C_{12} are from (4)), (in subscript m is for metastable phase and s for stable)

	a (Å)	b (Å)	c (Å)
$(C_{12})_m$	5.04	7.62	34.2
$(C_{15})_s$	5.13 ± 0.02	7.69 ± 0.01	42.3 ± 0.2

which is given elsewhere [12, 13]. In this case the subscript m refers to "maille", the french work for cell. Their values for four binary systems ($C_{12}-C_{15}$, $C_{12}-C_{13}$, $C_{13}-C_{14}$ and $C_{14}-C_{15}$) are reported in Table IV. Roughly, the difference between two unit cells (in this case of orthorhombic cells) is linked to the difference of chain length (the a and b parameters are quite the same). That explains why $\varepsilon^i_m(R_I)$ is higher for cases with $\Delta n = 1$ that for cases with $\Delta n = 3$.

Considering the function value at the equimolar fraction, we have $G^{E,\mathrm{sol}}(x = 1/2) = 800\,\mathrm{J \cdot mol^{-1}}$ for $C_{12}-C_{15}$. We compare in Table IV this value with that of another system $C_{12}-C_{13}$ [4]. These two systems have in common C_{12} and have a chain length difference respectively equal to 3 and 1. Increasing the chain length difference amounts to saying that, in the case of n-alkanes, we increase the melting temperature difference between the two components (ΔT(K)). Are also reported in the table different crystallographic and thermodynamic values of those systems such as: the width ℓ(K) of the melting domain of this R_I form at $x = 1/2$ (a eutectic for $C_{12}-C_{15}$ and a loop for the other systems) and, also, the degree of isomorphism $\varepsilon^i_m(R_I)$. The excess quantity $G^{E,\mathrm{sol}}(x = 1/2)$ for $C_{12}-C_{15}$ is three times bigger than that for $C_{12}-C_{13}$, which explains that we get a eutectic instead of a loop. This is again intrinsically linked to the large chain length difference and also to the large ℓ(K) difference (16 K instead of 2 K). Regarding the crystallographic values, the big chain length difference between the two molecules (Tab. III) leads to a degree of similarity very small (0.75 instead of 0.91).

TABLE IV Characteristic values of different studied systems in comparison with the present studied system $C_{12}-C_{15}$

	$\varepsilon^i_m(R_I)$	$\Delta T(K)$	$\ell(K)$	$G^{E,sol}(x = 1/2)$ $J \cdot mol^{-1}$
$(C_{12})_m-(C_{15})_s$	0.75	24.9	16.0	800
$(C_{12})_m-(C_{13})_s$	0.91	9.9	2.0	244
$(C_{13})_s-(C_{14})_m$	0.92	7.7	1.6	216
$(C_{14})_m-(C_{15})_s$	0.93	7.3	1.5	187

Let us consider, now, the two other binary systems ($C_{13}-C_{14}$ and $C_{14}-C_{15}$) with consecutive alkanes from C_{12} to C_{15} (that is to say all the intermediary odd–even or even–odd systems between C_{12} and C_{15}). The data are also reported in Table III. We increase, now, the chain length system by system, keeping constant the chain length difference ($\Delta n=1$). Compared to the first one ($C_{12}-C_{13}$), increasing the chain length leads to come closer to the thermodynamic ideality since, the excess function $G^{E,\mathrm{sol}}(x=1/2)$, ΔT and ℓ decrease towards 0. Regarding the degrees of isomorphism, the value is bigger for the three systems with $\Delta n=1$ than for $C_{12}-C_{15}$ where $\Delta n=3$.

In conclusion, large domains of miscibility, in cases of odd–even or even–odd systems, are obtained for two consecutive components and, furthermore, longer the chains are, more extend is the monophased R_I domain. For $C_{12}-C_{15}$ ($\Delta n=3$), the non miscibility in the solid state is largely explained both in terms of thermodynamic and crystallographic aspects. Even if only 40% of the stable [R_I + L] domain is accessible experimentally, the crystallographic-thermodynamic approach enables to fit the liquidus curve well enough. As far as the modelisation equilibrium for this system is concerned, further work is in progress on other binary systems to extend to $\Delta n=3$ the thermodynamic–crystallographic correlations given by Oonk *et al.* [11] on systems with $\Delta n=1$ and 2.

Acknowledgement

The authors gratefully thank Pr. H. A. J. Oonk for his help in the part of the thermodynamic interpretation.

References

[1] P. Espeau, H. A. J. Oonk, P. R. van der Linde, X. Alcobe and Y. Haget, *J. Chem. Phys.*, **92**, 747 (1995).
[2] F. Rajabalee, P. Espeau and Y. Haget, *Mol. Cryst. Liq. Cryst.*, **269**, 165 (1995).
[3] L. Robles, P. Espeau, D. Mondieig, Y. Haget and H. A. J. Oonk, *Thermochimica Acta*, **274**, 61 (1996).
[4] P. Espeau, *European Label Thesis*, University of Bordeaux I (1995).
[5] R. Courchinoux, N. B. Chanh, Y. Haget, T. Calvet, E. Estop and M. A. Cuevas-Diarte, *J. Chim. Phys.*, **86**(3), 561 (1989).
[6] J. Doucet, I. Denicolo, A. F. Craievich and C. Germain, *J. Chem. Phys.*, **80**(4), 1647 (1984).
[7] S. K. Filatov, E. N. Kotelnikoya and E. A. Aleksandrova, *Zeit. Krist.*, **172**, 35 (1985).
[8] M. H. G. Jacobs and H. A. J. Oonk, A computer program for the thermodynamic assessment of vapourus, liquidus, solidus curves in TX phase diagrams, version 1.2. Chemical Thermodynamics Group. Utrecht University (1989).
[9] H. A. J. Oonk, Phase theory: the thermodynamics of heterogeneous equilibria (Elsevier Science, Amsterdam, 1981).

[10] D. Mondieig, P. Espeau, L. Robles, Y. Haget, H. A. J. Oonk and M. A. Cuevas-Diarte, *J. Chem. Soc. Faraday Trans.*, **93**(18), 3343 (1997).
[11] H. A. J. Oonk, D. Mondieig, Y. Haget and M. A. Cuevas-Diarte, *J. Chem. Phys.*, **108**(2), 715 (1998).
[12] F. Michaud, *European Label Thesis*, University of Bordeaux I (1994).
[13] Y. Haget, L. Bonpunt, F. Michaud, P. Négrier, M. A. Cuevas-Diarte and H. A. J. Oonk, *J. Appl. Cryst.*, **23**, 492 (1990).